# Incorporation Of Tic Particulates On Aisi 4340 Low Alloy Steel Surfaces Via Tungsten Inert Gas Arc Melting

## S. Mridha[1], A.N Md Idriss[2] and T.N. Baker[3]

[1, 2]Advanced Materials and Surface Engineering Research Unit
Department of Manufacturing and Materials Engineering
International Islamic University Malaysia, P.O. Box 10, 50728, Kuala Lumpur, Malaysia
[3]Department of Mechanical Engineering
University of Strathclyde, Glasgow G1 1XJ, UK

[1]shahjahan@iium.edu.my; [2]nazrinidriss@yahoo.com; [3]neville.baker@strath.ac.uk

**Abstract:** Surface cladding utilizes a high energy input to deposit a layer on substrate surfaces providing protection against wear and corrosion. In this work, TiC particulates were incorporated by melting *single tracks* in powder preplaced onto AISI 4340 low alloy steel surfaces using a Tungsten Inert Gas (TIG) torch with a range of processing conditions. The effects of energy input and powder content on the melt geometry, microstructure and hardness were investigated. The highest energy input (1680 J/mm) under the *TIG torch* produced deeper (1.0 mm) and wider melt pools, associated with increased dilution, compared to that processed at the lowest energy (1008 J/mm). The melt microstructure contained partially melted *TiC particulates* associated with dendritic, cubic and globular type *carbides* precipitated upon solidification of TiC dissolved in the melt; TiC accumulated more near to the melt-matrix interface and at the track edges. Addition of 0.4, 0.5 and 1.0 mg/mm$^2$ TiC gave hardness values in the resolidified melt pools between 750 to over 1100Hv, against a base hardness of 300 Hv; hardness values are higher in tracks processed with a greater TiC addition and reduced energy input.

**Introduction:** Surface modifications are normally applied to increase wear and corrosion resistance, thus prolonging the shelf life and making the component competitive and better suited in terms of price and service applications. Among the processes employed for surface modification, incorporation of ceramic particles to produce a metal matrix *composite layer* is popular because this method can tailor the surface to suite the requirements of many applications. High energy *laser and electron beam* melting techniques are used extensively for processing such composite layers which are reported to increase wear and corrosion resistance significantly [1-5]. However, laser and electron beam surfacing techniques have a limited application because of the expensive establishment and precision control of the system. [6-9]. An alternative and *novel method* was developed using conventional TIG torch melting for surface modification work [10-12]. In this method, the TIG torch with adequate power density is scanned over the material which melts a thin layer of the substrate surface by absorbing heat energy from the torch in a short time interval; the melt matrix interface moves toward the substrate at a rate which depends on the scanning speed, and creates a melt pool. Upon solidification, the resolidified layer creates a metallurgical bond with the substrate material. This TIG surface melting process is simpler, requires cheaper establishment, is flexible in operation, economical in time, energy and manufacturing procedure compared to laser and electron beam processing. A limited number of publications based on TIG torch surfacing have been reported in the literature [13-18].

There are few reports in the literature of investigations to produce significant relationships between the processing conditions and the coating quality, especially on steel substrates. Such an experimental study was conducted at the Department of Manufacturing and Materials Engineering, IIUM, to incorporate TiC ceramic particulates on to a AISI 4340 low alloy steel surface, using a

powder preplacement technique and melting under a TIG torch. This paper describes the influences of processing conditions, such as energy input and *TiC addition* on the quality of processed layer, assessed in terms of adhesion, defects, uniformity in TiC distribution in the microstructure, and hardness development.

**Experimental:** TiC ceramic powder of 99.5% purity with the nominal size of 45-100 μm supplied by Cera TM Incorporated from Milwaukee, Winsconsin was used as reinforcing material on AISI 4340 low alloy steel substrate material of composition given in Table 1; the sample size was 100×40×15 mm, ground on emery paper and degreased in acetone, before preplacing TiC powder of 0.4, 0.5, 1.0 mg per millimetre square area of the sample surface using a PVA binder.

Table 1: Composition of AISI 4340 low alloy steel in wt% .

| C | Mn | Si | S | P | Cr | Ni | Mo | Fe |
|---|----|----|---|---|----|----|----|----|
| 0.38-0.43 | 0.60-0.80 | 0.15-0.30 | 0.04 | 0.035 | 0.70-0.90 | 1.65-2.00 | 0.20-0.30 | Bal. |

Preplaced powder samples were dried in an oven at $80^oC$ for 1 h to remove the moisture. Single phase TIG 165 was used to generate a torch using a 2.4mm dia thoriated W electrode. Single melt tracks were processed by scanning the torch with different energy inputs (Table 2) on preplaced powder substrate surfaces using a speed of 1 mm/s; the substrate was 1 mm below the electrode tip. The travelling direction and distance were controlled using a simple numerical control. All samples were shielded using streamed argon gas purged at 20 L/min to prevent excessive oxidation. Track topography was viewed under a Nikon Measuring Microscope mm-400/L. The polished cross section was chemically etched in a Nital solution for a period of 5 second. A Nikon Epiphot 200 optical microscope and a JEOL JSM 5600 scanning electron microscope were used to analyze the microstructure of selected samples. A Wilson Wolpert microhardness testing machine was used to determine the hardness of selected samples at 500 gf with 10 second delay. The heat input (H) for melting the track under the *torch generated* at 30 V and 70-110A current (I) and at 1 mm/s traversing speed (S), was calculated using Equation 1 [19], where η is the efficiency of heat absorption which is considered to be 48% for TiG torch melting. The calculated values for the processing conditions along with the amount of TiC powder employed in this investigation are presented in Table 2.

$$H = \eta \frac{VI}{S}$$

(1)

Table 2. Melting conditions and dimensions of the processed tracks

| Track No. | Voltage [V] | Current [A] | Speed [mm/s] | Energy [J/mm] | TiC added [mg/mm$^2$] | Melt depth [mm] | HAZ [mm] |
|-----------|-------------|-------------|--------------|---------------|------------------------|-----------------|----------|
| 1 | 30 | 70 | 1 | 1008 | 0.4 | 0.54 | 0.87 |
| 2 | 30 | 80 | 1 | 1152 | 0.4 | 0.70 | 0.97 |
| 3 | 30 | 90 | 1 | 1296 | 0.4 | 1.07 | 1.08 |
| 4 | 30 | 70 | 1 | 1008 | 0.5 | 0.51 | 0.84 |
| 5 | 30 | 80 | 1 | 1152 | 0.5 | 0.64 | 0.92 |
| 6 | 30 | 90 | 1 | 1296 | 0.5 | 0.79 | 1.01 |
| 7 | 30 | 110 | 1 | 1680 | 1.0 | 0.95 | 1.10 |

**Results and Discussion**

**Surface Topography:** The track surfaces were seen to be free from any cracks or visible defects. With 0.4 and 0.5 mg/mm$^2$ TiC additions at 1296 J/mm energy input, the surface became shiny and smooth with rippling marks; rippling marks were more evident in the track processed with 0.4 mg/mm$^2$ TiC (Fig.1a) compared to that with 0.5 mg/mm$^2$ TiC (Fig. 1b). Ripples were also observed

earlier in both laser TIG torch melted surfaces and they are suggested to have been caused by *fast freezing* of the fluid melt [2, 18]. Tracks with a smaller TiC addition showed more ripples, which are related to the generation of increased melt fluidity compared to more viscous melt found with a 0.5 mg /mm$^2$ TiC addition. Those tracks glazed with lower energy inputs and also higher TiC additions, created viscous melts and the rough surfaces; however, no defects were visible, Fig. 1c-d. Tracks produced with 1.0 mg/mm$^2$ TiC additions and glazed at 1152 J/mm gave very rough and dull surfaces, Fig. 1d, and the surface appeared un-melted, but free from any visible defects. In the absence of any molten surface, no ripple marks were observed in any of the tracks.
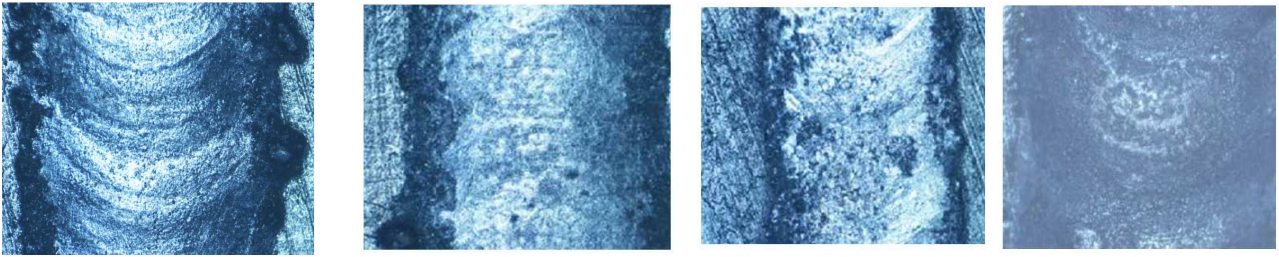


Fig. 1 Topography of tracks processed at: (a) 1296 J/mm with 0.4 mg/mm$^2$ TiC (b) 1296 J/mm with 0.5 mg/mm$^2$ TiC, (c) 1008 J/mm with 0.4 m/mm$^2$g TiC and (d) 1152 J/mm with 1.0 mg/mm$^2$ TiC.

**Melt Configuration and Microstructure:** The cross sectional view of the track processed under the present processing conditions with additions of 0.4, 0.5 and 1.0 mg/mm$^2$ TiC gave a *hemispherical* shape melt pool, Fig. 2. The melt microstructure consists of partially melted TiC particulate, which concentrated near to the melt-matrix interface (Figs. 2a-c) and more at the edges (Figs. 2a-d). Because of the energy distribution pattern of the beam (may be *Gaussian* type as for a laser beam), the melt pool was hemispherical in shape and *agglomeration of TiC* at the edges which are commonly observed in laser processing [2], and also in TIG surfacing work [14, 17, 18]. The convectional flow of the melt is believed to have distributed TiC particulates towards the bottom of the melt. Since heat dissipation from the liquid melt is more from melt-matrix interface than from the top surface, more TiC particulates are found near to the interface; low energy glazing at the edges created low temperature viscous melt and hence more TiC agglomeration in these regions (Fig. 2d).
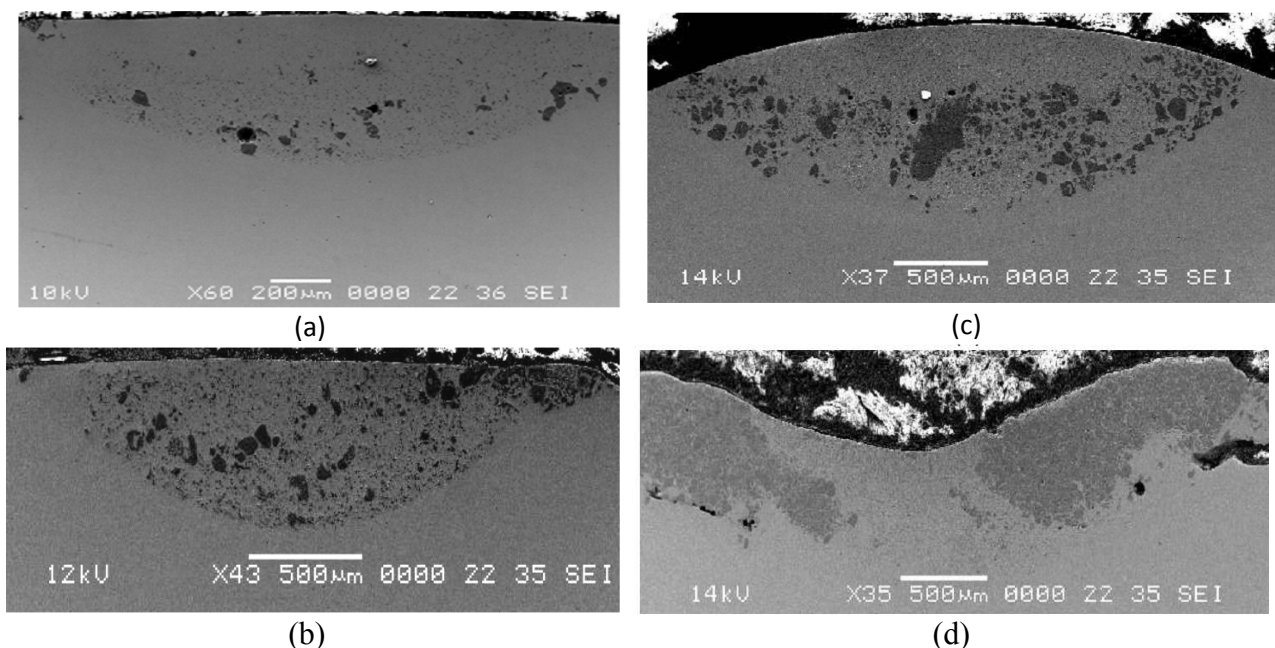


Fig. 2 Melt cross sections (a) 1008 J/mm, 0.4 mg/mm$^2$, (b) 1008 J/mm, 0.5 mg/mm$^2$, (c) 1680 J/mm, 1.0 mg/mm$^2$ and (d) 1152 J/mm, 1.0 mg/mm$^2$

The middle regions of the tracks melted most of the TiC particulates and dissolved into the substrate liquid melt. This happened because of the energy intensity of the beam, which is highest at the centre zone. The melting of TiC depends both on energy input and TiC content, together with size of the TiC particulate. High energy input tracks with 0.4 mg/mm$^2$ TiC dissolved more TiC (Fig. 2a), while less was dissolved with 1.0 mg/mm$^2$ TiC, even when glazed at 1680 J/mm, Fig. 2c. TiC particulates in the melt are found to have cracks and even *fragmentation*, especially in the larger particulates (Fig. 3a), and these are believed to be the result of thermal shock associated with fast heating during the glazing operation. The melt layer containing dissolved TiC, resolidified by precipitation of mostly globular type particles (Fig. 3b); *dendrites* are also seen in several areas (Fig. 3c), as are flower-type dendrites and cubic particles. These types of microstructures are also reported by other researchers [4, 16, 17]. Precipitation of these particles occurred by dissolution of TiC, as evident from Fig. 3d, where *globular* particles precipitated adjacent to the TiC ceramic particulate and the cubic type away from it. The present observations are supported by previous laser works in literatures [2, 20]. All these particles were analysed as carbides containing titanium, iron and molybdenum, Figs. 3e-f. The sizes of the precipitated carbides and their concentrations are greater in the high temperature regions of the melt and less so in other areas.

**Pores and defects:** All the tracks processed in this work were free from any cracks but pores were seen in the melt cross sections of some tracks. The pores are mostly in the low temperature regions of the melt pool and near to the melt-matrix interface. Pore formation is observed in most surface modification research which used powder preplacement and melting techniques [1, 2, 13, 18, 20]. The pores are bigger when glazed at a low energy input or after the addition of a larger amount of TiC powder (Figs. 2b-d). Formation of pores is reported to occur by *entrapment of gas* produced by burning the binder during the glazing operation [13, 18]. More pores develop in a viscous melt, especially near the melt-matrix interface and at the track edges. Glazing with a high energy beam and with a low TiC addition, created a highly fluid melt through which gas escaped easily during slow rates of solidification, resulting in a reduction in track porosity (Fig. 2a). However, reducing the amount of *binder* used in the powder preplacement process can help to minimise or eliminate pores entirely.
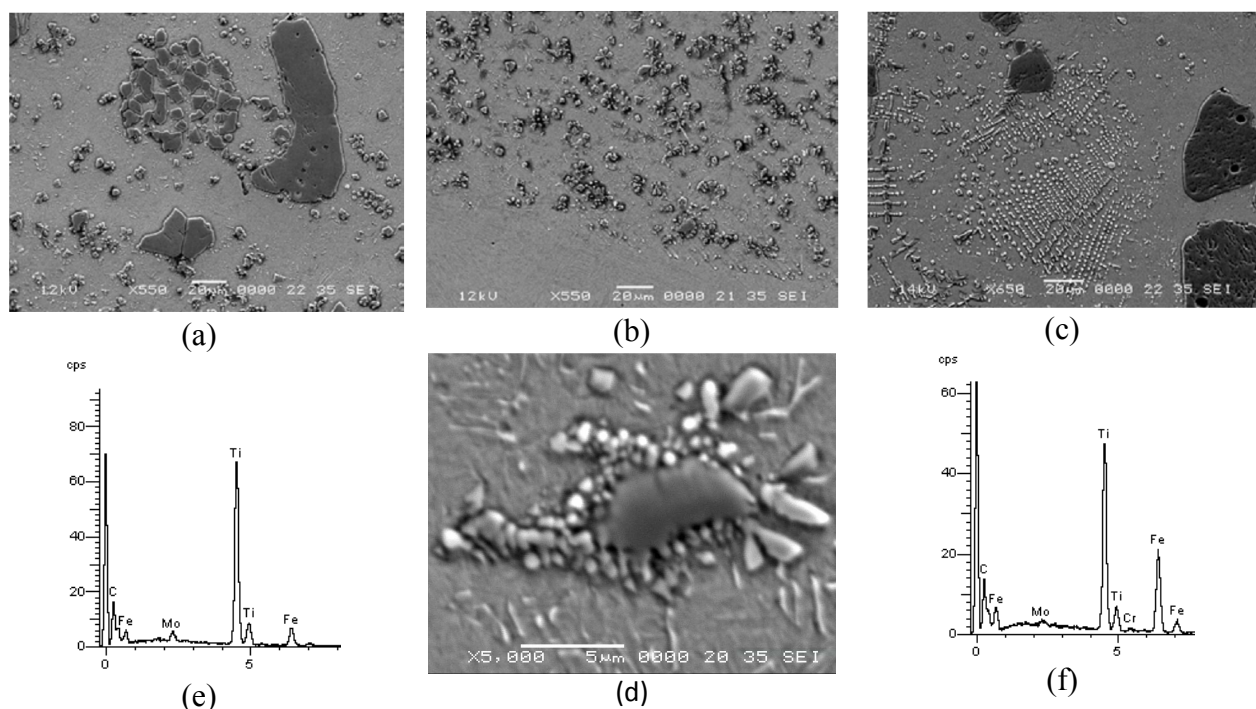

(a)


(b)


(c)


(e)


(d)


(f)

Fig. 3: (a) Fragmentation of TiC, (b) Carbide precipitates, (c) Dendrites from melt, (d) Precipitation of carbide from TiC dissolution, (e) EDS from cubic type particle and (f) EDS from globular particle.

**Melt dimension:** The depths of the *melt zone* and HAZ given in Table 2 show that the dimensions of these zones depend on the energy input and the amount of the TiC addition. When glazing is undertaken at 1296 J/mm, both the HAZ and the melt zone of the tracks containing 0.4 and 0.5 mg/mm$^2$ TiC are the largest; they are about 1.0 mm each, though the melt depth is 0.79 mm for the 0.5 mg.mm$^2$ TiC addition track. The geometric size of the melt pool, together with the heat affected zone, decreases with a reduced energy input, which is in agreement with other published research [13, 18. 20]. The greater energy absorption from high heat intensity glazing produced melting and created a high temperature melt, resulting in a reduction in the solidification rate. This reduced solidification rate helped in moving the melt-matrix interface towards the substrate, producing larger melt depth. Under this condition, the heat dissipation of the melt occurred by conduction through the substrate, which gave a greater depth of the martensitic HAZ microstructure. It can be seen that increasing the powder addition under the same energy input, reduced the depth of both the melt and the HAZ. With the 1.0 mg/mm$^2$ TiC powder addition, the melt size developed was comparable with those of other tracks *of greater melt depth*, but glazing using  the highest energy input (1680 J/mm) , resulted  in the  heat dissipation from the base metal taking place over a  longer time and  creating the deepest HAZ.

**Hardness measurement:** The depth hardness profiles of the tracks containing different TiC additions and processed under various energy inputs are shown in Figs. 4 and 5. The results show that the variation of hardness can be distinguished at the melt zone and HAZ region. The tracks processed with 0.4 (Fig. 4) and 0.5 mg/mm$^2$ (Fig.5) TiC additions using  a low energy input gave higher hardness values compared to those glazed at higher energy inputs. The track glazed with 1.0 mg/mm$^2$ TiC produced the highest hardness (Fig. 5), even though it was glazed with highest energy input of 1680 J/mm used in the present study. This happened because of the melt microstructure contained a higher TiC concentration (Fig. 2c) compared to other tracks, see Fig. 2. Under low energy input glazing, the melt pools will be smaller, which may be the reason for the *high hardness* values compared to those tracks processed at higher energy inputs. Glazing at 1296 J/mm energy input, with 0.4 and 0.5 mg/mm2 TiC additions generated more dilution, causing less dispersion of the TiC particles (Fig. 2a, b) which may be the reason for low hardness development for these tracks. The high *dissolution of TiC* particulates may have also contributed to decrease these hardness values. The measured hardness values in tracks containing thinly distributed TiC particulates, have smaller melt and heat affected zones compared to those tracks glazed at a low processing energy input. However, with the incorporation of TiC particulates, the maximum hardness in the melt zone increased from 700 to over 1100 Hv, depending on the processing conditions and the profile is shallow; the corresponding hardness of the  martensitic HAZ varies between 500 to 700 Hv, compared to the base steel substrate  hardness of 300 Hv.
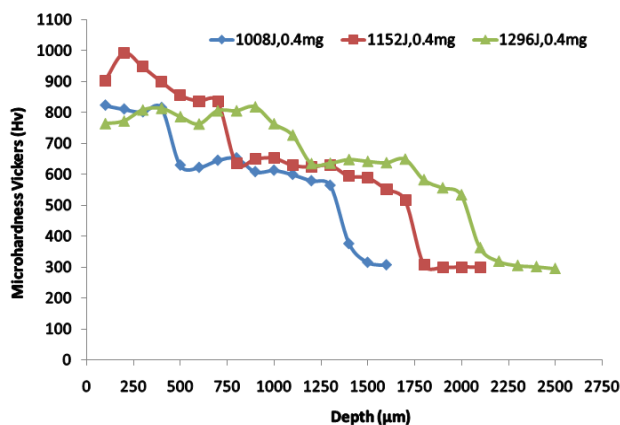


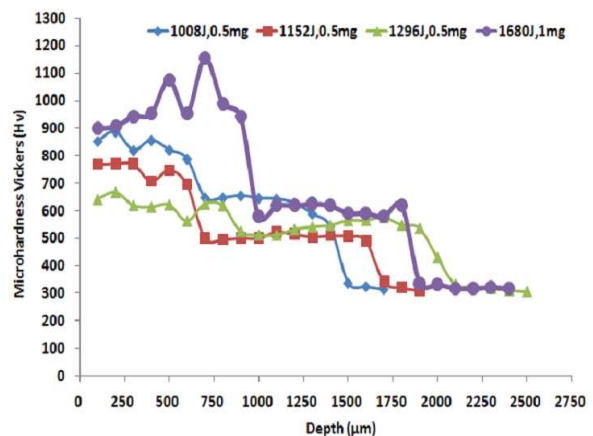Fig. 4 Hardness profiles of 0.4 mg/mm$^2$ TiC tracks

Fig. 5 Hardness profiles of 0.5 and 1.0 mg/mm$^2$ TiC tracks

**Conclusions** Crack free composite layers of 0.5 to 1.0 mm thickness were produced successfully on AISI4340 steel surfaces using a TIG torch technique to melt single tracks incorporating preplaced TiC particulates of nominal size 45-100μm. The melt pool was hemispherical in shape and the microstructure contained partially melted TiC particulates, precipitated globular and cubic type carbides together with dendrites. Some porosity was present. The concentration of TiC particulates was greater near to the melt matrix interface and at the track edges. Glazing at a low energy input, 1008 J/mm, combined with a high TiC addition, 0.5 mg/mm$^2$, produced a melt pool with a dense distribution of TiC particles. The maximum hardness in the processed composite layer is about 2.5 to 4 times the base hardness of 300 Hv, depending mainly on the processing conditions.

**References**

[1] J. H. Abboud and D.R.F. West, Journal of Materials Science Letters, **10**(19) (1991) p. 1149.

[2] S. Mridha and T.N. Baker, Journal of Materials Processing Technology, 2007. **185**(1-3): p. 38.

[3] M. J. Chao et al., Surface and Coatings Technology, 2008. **202**(10): p. 1918-1922.

[4] X. H. Wang et al., Surface and Coatings Technology, 202(15) (2008) p. 3600.

[5] H.-g. L. Kai-jin Huang and Zhou Chang-rong, Advance Materials Research. 179-180 **(**2011) p. 757.

[6] C. Pfohl and K. T. Rie, Surface and Coating Technology, 116-119 (1999) p. 911.

[7] X, Lifang, M. Xinxin and S. Yue, Wear, 246 No. 1-2 (2000) p. 40.

[8] W. Liang and X. G. Zao, Scripta Materialia, 44 (2002), p. 1049.

[9] J. Oh and S. Lee, Surface and Coatings Technology, 179 (2004) p. 340.

[10] S. Mridha, H. S. Ong, L. S. Poh and P. Cheang, Journal of Materials Processing Technolog, 113 (2001) p. 516.

[11] S. Baytoz, M. Uttran and M. Mustafa, Applied Surface Science, 252 (2005) p. 1313.

[12] D. Wenbin, J. Haiyan, Z. Xiaoqin, L. Dehui, and Y. Shoushan, Journal of Alloy and Compounds, 429 (2007) p. 233.

[13] S. Mridha and B. S. Ng, Surface Engineering, **15** (1999) p. 210

[14] X. H. Wang et al., Materials Science and Engineering: A, **441**(1-2) (2006) p. 60.

[15] X. H. Wang et al., Surface and Coatings Technology, **201**(12) (2007) p. 5899.

[16] Z. J. A. C. Zhang, Advance Material Research, **97-101** (2010) p. 1377.

[17] Li Mei Wang and J. B. L. Chi Yuan, Material Science Forum, **675-677** (2011) p. 783.

[18] S. Dyuti, S.Mridha., S. K. Shaha, Advanced Materials Research. **264-265** (2011) p. 1433.

[19] K. E. Easterling, Introduction to Physical Metallurgy of Welding, Butterworth-Heinemann, London (1992).

[20] T. N. Baker, H. Xin, C. Hu, and S. Mridha, Materials Science and Technology, 10 (1994) p.536.

**Incorporation of TiC Particulates on AISI 4340 Low Alloy Steel Surfaces via Tungsten Inert Gas Arc Melting**